



HAL
open science

Self-Standing Covalent Organic Framework Membranes for H₂/CO₂ Separation

Baoju Li, Zitao Wang, Zhuangzhuang Gao, Jinquan Suo, Ming Xue, Yushan Yan, Valentin Valtchev, Shilun Qiu, Qianrong Fang

► **To cite this version:**

Baoju Li, Zitao Wang, Zhuangzhuang Gao, Jinquan Suo, Ming Xue, et al.. Self-Standing Covalent Organic Framework Membranes for H₂/CO₂ Separation. *Advanced Functional Materials*, 2023, 33 (16), pp.2300219. 10.1002/adfm.202300219 . hal-04270597

HAL Id: hal-04270597

<https://hal.science/hal-04270597v1>

Submitted on 4 Nov 2023

HAL is a multi-disciplinary open access archive for the deposit and dissemination of scientific research documents, whether they are published or not. The documents may come from teaching and research institutions in France or abroad, or from public or private research centers.

L'archive ouverte pluridisciplinaire **HAL**, est destinée au dépôt et à la diffusion de documents scientifiques de niveau recherche, publiés ou non, émanant des établissements d'enseignement et de recherche français ou étrangers, des laboratoires publics ou privés.

DOI: 10.1002/ ((please add manuscript number))

Article type: Communication

Self-Standing Covalent Organic Framework Membranes for H₂/CO₂ Separation

Baoju Li, Zitao Wang, Zhuangzhuang Gao, Jinqian Suo, Ming Xue, Yushan Yan, Valentin Valtchev, Shilun Qiu, and Qianrong Fang**

B. Li, Z. Wang, Z. Gao, J. Suo, Prof. S. Qiu, Prof. Q. Fang

State Key Laboratory of Inorganic Synthesis and Preparative Chemistry, Jilin University,
Changchun 130012, P. R. China

E-mail: qrfang@jlu.edu.cn

Prof. M. Xue

School of Chemical Engineering and Technology, Sun Yat-sen University, Zhuhai 519082,
P. R. China

E-mail: xueming5@mail.sysu.edu.cn

Prof. Y. Yan

Department of Chemical and Biomolecular Engineering, Center for Catalytic Science and
Technology, University of Delaware, Newark, DE 19716, USA

Prof. V. Valtchev

Qingdao Institute of Bioenergy and Bioprocess Technology, Chinese Academy of Sciences
189 Song Ling Rd, Qingdao, Shandong 266101, China; Normandie Univ, ENSICAEN,
UNICAEN, CNRS, Laboratoire Catalyse et Spectrochimie, 6 Marechal Juin, 14050
Caen, France

Keywords: Covalent organic framework, self-standing membrane, H₂/CO₂ separation

Abstract: Covalent organic frameworks (COFs) have been proposed as promising candidates for engineering advanced molecular sieving membranes due to their precise pore sizes, modifiable pore environment, and superior stability. However, COFs are insoluble in common solvents and do not melt at high temperatures, which presents a great challenge for the fabrication of COF-based membranes (COFMs). Herein, for the first time, we report a new synthetic strategy to prepare continuous and intact self-standing COFMs, including 2D N-COF membrane and 3D COF-300 membrane. Both COFMs show excellent selectivity of H₂/CO₂ mixed gas (13.8 for N-COF membrane and 11 for COF-300 membrane), and especially ultrahigh H₂ permeance (4319 GPU for N-COF membrane and 5160 GPU for COF-300 membrane), which is superior to those of COFMs reported so far. It should be noted that the overall separation performance of self-standing COFMs exceeds the Robeson upper bound. Furthermore, a theoretical study based on Grand Canonical Monte Carlo (GCMC) simulation is performed to explain the excellent separation of H₂/CO₂ through COFMs. Thus, this facile preparation method will provide a broad prospect for the development of self-standing COFMs with highly efficient H₂ purification.

As the problems of global warming and environmental degradation become more and more serious, it is urgent to reduce carbon emissions and utilize clean energy.^[1] Hydrogen is one of the most promising alternative energy sources due to its high energy efficiency and zero-carbon emission, yielding only water when burned. At present, the most commonly used hydrogen production technology is steam reforming of methane and the subsequent water-gas shift (WGS) reaction, in which carbon dioxide is the main by-product.^[2] In order to obtain high purity hydrogen, it is necessary to find an efficient separation process of hydrogen and carbon dioxide, which is typical of pre-combustion capture. Compared with traditional separation processes, such as distillation, adsorption, extraction and crystallization, membrane-based separation is recognized as a powerful technology that guarantees high selectivity, low energy consumption and a small footprint for the separation process, satisfying the need for a new sustainable industrial process.^[3-5] Therefore, using membrane separation technology to purify hydrogen and capture carbon dioxide is one of the most promising means but still remain elusive.

Covalent organic frameworks (COFs) are two-dimensional (2D) or three-dimensional (3D) open networks precisely woven by organic building units through covalent bonds to constitute predesignate topologies and tunable pore structures, presenting an emerging class of crystalline porous polymers.^[6, 7] COFs have potential applications in many fields, such as catalysis,^[8] energy storage,^[9] sensing,^[10] photoelectric,^[11] gas storage,^[12] and separation,^[13] because of their ordered and tunable pore structures, permanent porosity with a large surface areas, facilely tailored functionalities, outstanding thermal stability, and specific adsorption affinities.^[14] It can be predicted that, amorphous membranes show uneven pores and a large amount of inaccessible pore volume, which will greatly affect their separation properties. On the contrary, due to the uniform channel sizes and more accessible functional sites, COF-based membranes (COFMs) are more likely to break through the trade-off between permeance and selectivity. Therefore, more and more scholars have currently made contributions to the development of COFMs.^[15-23] For instance, to enable COFMs to meet the needs of gas separation, some effective strategies have been developed, including multilayer membranes,^[24-26] vertical membranes,^[27] confined growth of metal-organic framework (MOF) inside a supported COF layer,^[28] and staggered stacking in 2D COF nanosheets for reducing the pore size.^[29] However, COFs are insoluble in common solvents and do not melt at high temperatures, which presents a great challenge for the fabrication of COFMs. There are still few truly universal approaches to make COFMs up to now. The classical method is to grow denser COFMs in situ on a modified porous substrate by a solvothermal reaction.^[30-32] Other methods

include interfacial polymerization,^[17,23] layer-by-layer stacking of nanosheets,^[18] electrophoretic deposition,^[33] diffusion-induced,^[34] baking,^[35] and a compressed imine-based COF-aerogel.^[36] It is worth noting that most of the reported membranes are fabricated on a support, and they cannot make full use of the pore of COF itself due to the shielding effect of other phases.^[37] Therefore, the development of a new method for synthesizing self-standing COFMs is of great significance for making full use of the rich structural advantages of COFs.

Herein, we report a new strategy to construct continuous and intact self-standing COFMs for H₂/CO₂ separation, including 2D N-COF and 3D COF-300 membranes. Furthermore, these membranes exhibit high selectivity of H₂/CO₂ mixed gas with 13.8 for N-COF membrane and 11 for COF-300 membrane as well as excellent H₂ permeance of 4319 GPU for N-COF membrane and 5160 GPU for COF-300 membrane, and especially the H₂ permeance for COF-300 membrane is higher than those of previous reports from other COF-based membranes. Notably, the overall separation performance of both COFMs exceeds the Robeson upper bound, and a theoretical study based on Grand Canonical Monte Carlo (GCMC) simulation further demonstrates the high separation power of COFMs in the H₂/CO₂ separation. To the best of our knowledge, it represents the first case of self-standing COFMs for H₂/CO₂ separation, which will greatly promote the development of COFMs for highly efficient H₂ purification.

To obtain high-quality self-standing COFMs, we developed an ammonium acetate-assisted steam induction strategy (Scheme 1). Typically, the appropriate proportions of amine and aldehyde organic linkers were mixed evenly in the first step. Subsequently, an appropriate amount of ammonium acetate was added and grind evenly with a mortar. In this process, a few drops of water were added dropwise to form a solid-liquid blend, and the bubbles were removed by ultrasound. The resultant blend was put into a round mold with a depth of 1 mm and a diameter of 15 mm, and was pressed flat with a glass sheet. Finally, the mold was put into a stainless-steel autoclave without contacting with dioxane and acetic acid solution directly, and reacted at 120 °C for 72 h. Notably, ammonium acetate will gradually decompose in the process of COFMs formation, providing enough space for the organic block reaction to obtain high-quality COFMs. The resultant COFMs were gently rinsed with acetone (3 × 3.0 mL) and dioxane (3 × 3.0 mL) to remove potentially unreacted organic linkers, and then vacuum-dried overnight at 100 °C (Figure S1, Supporting Information).

The X-ray powder diffraction (PXRD) and grazing incidence X-ray diffraction (GIXRD) patterns of the fabricated COFMs showed typical crystal material characteristics, confirming a highly crystalline nature (Figure 1a and 1b and Figure S2, Supporting Information). These peak positions match with the crystal structures simulated by the Materials Studio 7.0 software.^[38] It

can be seen the absence of peaks at 1571 cm^{-1} and 1413 cm^{-1} from the Fourier-transform infrared (FT-IR) spectra (Figure S3, Supporting Information), indicating the complete removal of the ammonium acetate from COFMs. The C=O stretching vibration at around 1695 cm^{-1} and N-H stretching vibration at around $3100\text{-}3400\text{ cm}^{-1}$ were almost disappeared. Meanwhile, the new peaks of C=N bonds were displayed at around 1620 cm^{-1} and 1200 cm^{-1} , demonstrating that the Schiff-base condensation reaction occurred. Scanning electron microscope (SEM) images indicated that their surfaces were continuous and free of defects (Figure 1c and 1d), which is particularly important for the selectivity of the separation. At the same time, the underlying crystals showed lots of pinholes from the decomposition of ammonium acetate and the agglomeration of COF microcrystals, which will greatly increase the mass transfer of channels. The thickness of both COFMs was about $800\text{ }\mu\text{m}$, in which the part for dense membranes is only about $1\text{ }\mu\text{m}$ and the rest of membranes is mesoporous or macro-porous. (Figure 1e and 1f as well as Figures S4 and S5, Supporting Information). Thermogravimetric analysis (TGA) profiles showed that no significant mass loss was observed for COFMs under a high temperature of $400\text{ }^{\circ}\text{C}$ (Figure S6, Supporting Information).

In order to verify the porosity and surface areas of self-standing COFMs, N_2 adsorption-desorption tests were carried out at 77 K . The N_2 -adsorption isotherms exhibited classic type-I isotherms characterized by a sharp uptake under low relative pressures in the range of $P/P_0 = 10^{-5}\text{-}10^{-2}$ (Figure S7, Supporting Information). The Brunauer–Emmett–Teller (BET) surface areas were found to be $845\text{ m}^2/\text{g}$ for N-COF membrane and $834\text{ m}^2/\text{g}$ for COF-300 membrane, respectively (Figure S8, Supporting Information). The pore size distribution of COFMs was calculated by nonlocal density functional theory (NLDFT, Figure S9, Supporting Information), and the pore diameters of N-COF and COF-300 membranes are 5.9 \AA and 8.6 \AA respectively, which is consistent with the previous reports.^[39, 40]

In the process of gas separation, the adsorption between the membrane material and the gas has a very important influence on the separation performance. Therefore, we investigated the adsorption isotherms of H_2 , CO_2 and CH_4 for two COFMs at different temperatures (Figure S10, Supporting Information). In previous report, COF-300 had the strongest adsorption effect for CO_2 with the isosteric heat of adsorption (Q_{st}) of 33 KJ/mol , CH_4 with the Q_{st} of 29 KJ/mol , and H_2 with the Q_{st} of 7 KJ/mol , respectively.^[26] Meanwhile, we carried out CO_2 and CH_4 adsorption tests of N-COF at 273 K and 298 K , whereas the H_2 isotherms were collected at 77 K and 87 K because the adsorption behavior of N-COF for H_2 was not obvious under the condition of 298 K . Subsequently, the Q_{st} was calculated by the Clausius-Clapeyron method. The Q_{st} value of N-COF for CO_2 was 39.7 KJ/mol , which is much higher than those of H_2 (7.4

KJ/mol) and CH₄ (20.7 KJ/mol). Both COFMs showed strong adsorption of CO₂ originating from the Lewis acid-base interaction of CO₂ with abundant imine bonds in the porous frameworks of the COFs. This specific adsorption may have important guiding significance for gas separation performance.

Encouraged by the above results, we tested their H₂/CH₄ and H₂/CO₂ separation performance using the Wicke–Kallenbach system with an equimolar binary gas mixture as the feed and the Ar as the sweep gas on the permeate side at room temperature (25 °C). To avoid the risk of back flow of sweep gas during separation tests, an absolute pressure difference of about 0.1 bar across the membrane was used in this study (i.e., the feed pressure was fixed at about 1.1 bar of absolute pressure and the sweep pressure was kept at 1 atm, Figure S11, Supporting Information). As shown in Figure 2a, the selectivity of N-COF membrane for H₂/CO₂ is 13.8 with the permeance of H₂ of 4319 GPU, and the selectivity for H₂/CH₄ is 5.8 with the permeance of H₂ of 4634 GPU. Similarly, the selectivity of COF-300 membrane for H₂/CO₂ is 11 with the permeance of H₂ of 5160 GPU, and the selectivity for H₂/CH₄ is 5 with the permeance of H₂ of 5637 GPU (Figure 2b). Remarkably, the selectivity of two COFMs for H₂/CO₂ and H₂/CH₄ was higher than that of the corresponding Knudsen diffusion (H₂/CO₂: 4.7; H₂/CH₄: 2.8). Although the kinetic diameter of CO₂ is smaller than that of CH₄, both membranes showed even higher H₂/CO₂ selectivity, which indicates that the molecular sieving effect does not dominate the separation process. As reported previously,^[41-43] this phenomenon can be explained by the synergistic effect of adsorption and diffusion of gas in the membranes instead. When the gas mixture passes through the two self-standing membranes, only CO₂ can be retained in the pore structure of the membranes while other small gas molecules will easily permeate through the framework since imine-based COFMs show a strong adsorption of CO₂. That is to say, the mobility of CO₂ was retarded by this strong adsorption, while H₂ can still pass through the pore network easily, leading to a high H₂/CO₂ selectivity. Notably, both COFMs also have very high H₂ permeance, the possible reasons are as follows: (1) both COFMs have large intrinsic pore sizes, which facilitate the rapid transport of gas molecules; (2) the self-standing membrane structure is not shielded by other phases, and there are abundant large pores stacked between crystals in the interior of the membrane, which also provide mass transfer channels for gas diffusion. Therefore, this unique membrane structure contributes to the high gas permeance of these self-standing membranes. When the transmembrane pressure difference is increased up to 0.2 bar, the selectivity of the N-COF membrane for H₂/CO₂ has been extremely reduced even below the Knudsen diffusion. Furthermore, the selectivity can be restored when the pressure is dropped to 0.1 bar, which indicates that the N-COF membrane

still maintains structural integrity. The performance decline can be attributed to the low adsorption effect that is not enough to hinder the diffusion of CO₂ under a high pressure.

Both COFMs exhibited outstanding running stability, which is reflected in the fact that the membranes have almost no performance degradation after 72 h of continuous testing (Figure 2c and 2d). In addition, the separation tests were also carried out at 60 °C and 100 °C. As the temperature increases, the H₂ permeance of two COFMs is almost unchanged, while the selectivity of H₂/CO₂ could be maintained at 12.2 and 10.6 for N-COF membrane and at 10 and 9 for COF-300 membrane, respectively (Figure 2e and 2f). This trend can be explained by the interplay of adsorption and diffusion of H₂ and CO₂ in the pore structures of two self-standing COFMs. As the temperature increases, CO₂ can diffuse more easily in the resulting free volume, which leads to an enhancement of CO₂ permeance and hinders the diffusion of H₂. It may be because these COFMs still have a strong adsorption effect of CO₂ at high temperature, so the separation of H₂/CO₂ by two COFMs showed a good temperature stability and their separation performance did not decrease after running for 60 h at different temperatures (Figure S12, Supporting Information). The temperature dependence of H₂ and CO₂ permeance can be described by the Arrhenius equation (Figure S13, Supporting Information), indicating that the diffusion process of CO₂ in two COFMs is mainly activated diffusion. While the constant H₂ permeance of two membranes showed a weak dependence on temperature, this may be because the competitive diffusion of CO₂ at high temperature hinders the penetration of H₂. Moreover, after long-term testing at different temperatures, both COFMs kept its crystalline and structurally intact, which could be determined by PXRD tests (Figure S14, Supporting Information).

We summarized the permeance and selectivity of all reported COFMs for H₂/CO₂ (Table S1, Supporting Information). Both self-standing COFMs exhibited excellent selectivity, which considerably exceeds the corresponding Knudsen constants (4.7). In particular, both self-standing COFMs showed ultrahigh H₂ permeance, which is superior to those of COFMs reports up to now, such as COF-LZU1 (3684 GPU)^[24] and vertically aligned TFB-BD (3802 GPU).^[27] Furthermore, the overall performance of both self-standing COFMs surpasses the Robeson upper bound for H₂/CO₂ gas pairs (Figure 3, black line).^[44] Notably, these self-standing COFMs exhibit high values for both permeance and selectivity, demonstrating an antitrade-off phenomenon. This is because self-standing COFMs are entirely composed of COFs without any interference from any secondary phase, ensuring high separation efficiency. The high permeance is also an inherent characteristic of these self-standing membranes since the cavities are inevitably formed in the membranes during the crystallization process, ensuring that the

COFMs exhibit abundant CO₂ adsorption sites and mass transfer channels. Therefore, COFMs show high flux and selectivity in the process of separating H₂/CO₂, despite their relatively thicker layer compared to the other composite membranes with the shielding effect of other phases or zigzag pathways.^[27]

We further performed a theoretical calculation to explain the separation of H₂/CO₂ by COFM materials. Grand canonical Monte Carlo (GCMC) simulation by the Sorption module of Materials Studio was used to simulate the competitive adsorption of CO₂/H₂ at fixed pressure.^[45] The partial pressure of CO₂ and H₂ were set to be 50 kPa and the temperature was set at 298 K. The energy forcefield of Universal was utilized. The van der Waals interactions were calculated by the atom-based method with a fine cutoff distance of 12.5 Å, whereas the Ewald and group method summed the Coulombic interactions. The simulation parameters were set as 5 × 10⁶ equilibration steps and 5 × 10⁷ production steps. The 1 × 1 × 3 supercell of COF-300 and 2 × 2 × 5 supercell of AB stacking N-COF were used as adsorbents. The results showed that, in COF-300 cells, CO₂ molecules tended to locate between the p-benzaldehyde structural units, whereas H₂ molecules were dispersed in the open channels (Figure 4a). The average molecule loading in the supercell was 0.5 for H₂ and 4.9 for CO₂. The average isosteric heat was 7.1 kJ/mol for H₂ and 16.5 kJ/mol for CO₂. In this way, CO₂ molecules were adsorbed in the stacked pores, and H₂ molecules could flow in the pores, which explains why COF-300 has a large pore size but can still effectively separate CO₂ and H₂. Similarly, the average molecule loading in the AB stacking N-COF supercell was 4.2 for H₂ and 82.7 for CO₂ (Figures 4b and S15, Supporting Information). The average isosteric heat was 2.7 kJ/mol for H₂ and 6.7 kJ/mol for CO₂. Therefore, GCMC simulation results illustrated that both COFMs had high adsorption capacity for CO₂ and relatively weak adsorption behavior for H₂, leading to the excellent separation property of H₂/CO₂.

In conclusion, we developed a new universal method for preparing two self-standing COFMs for the first time, 2D N-COF membrane and 3D COF-300 membrane, and applied these COFMs to the separation of H₂/CO₂ gas pairs. The results showed that both self-standing COFMs exhibited outstanding selectivity for H₂/CO₂ mixed gas (13.8 for N-COF membrane and 11 for COF-300 membrane), and ultrahigh H₂ permeance (4319 GPU for N-COF membrane and 5160 GPU for COF-300 membrane) based on the separation mechanism of adsorption diffusion, which is of great industrial importance for gas separation applications. In addition, the obtained membranes have excellent thermal stability and a long-term cycle stability, and their overall separation performance exceeds the Robeson upper bound. Furthermore, a theoretical simulation based on Grand Canonical Monte Carlo method is studied to illustrate

the separation of H₂/CO₂ based on COFMs. Thus, this facile preparation strategy will provide a broad outlook for developing COFMs with highly efficient separation of H₂/CO₂ or other gas pairs in the future.

Supporting Information

Supporting Information is available from the Wiley Online Library or from the author.

Acknowledgements

This work was supported by National Key R&D Program of China (2022YFB3704900 and 2021YFF0500500), National Natural Science Foundation of China (22025504, 21621001, and 22105082), the SINOPEC Research Institute of Petroleum Processing, "111" project (BP0719036 and B17020), China Postdoctoral Science Foundation (2020TQ0118 and 2020M681034), and the program for JLU Science and Technology Innovative Research Team. V.V., Q.F. and S.Q. acknowledge the collaboration in the framework of China-French joint laboratory "Zeolites".

Conflict of Interest

The authors declare no conflict of interest.

Received: ((will be filled in by the editorial staff))

Revised: ((will be filled in by the editorial staff))

Published online: ((will be filled in by the editorial staff))

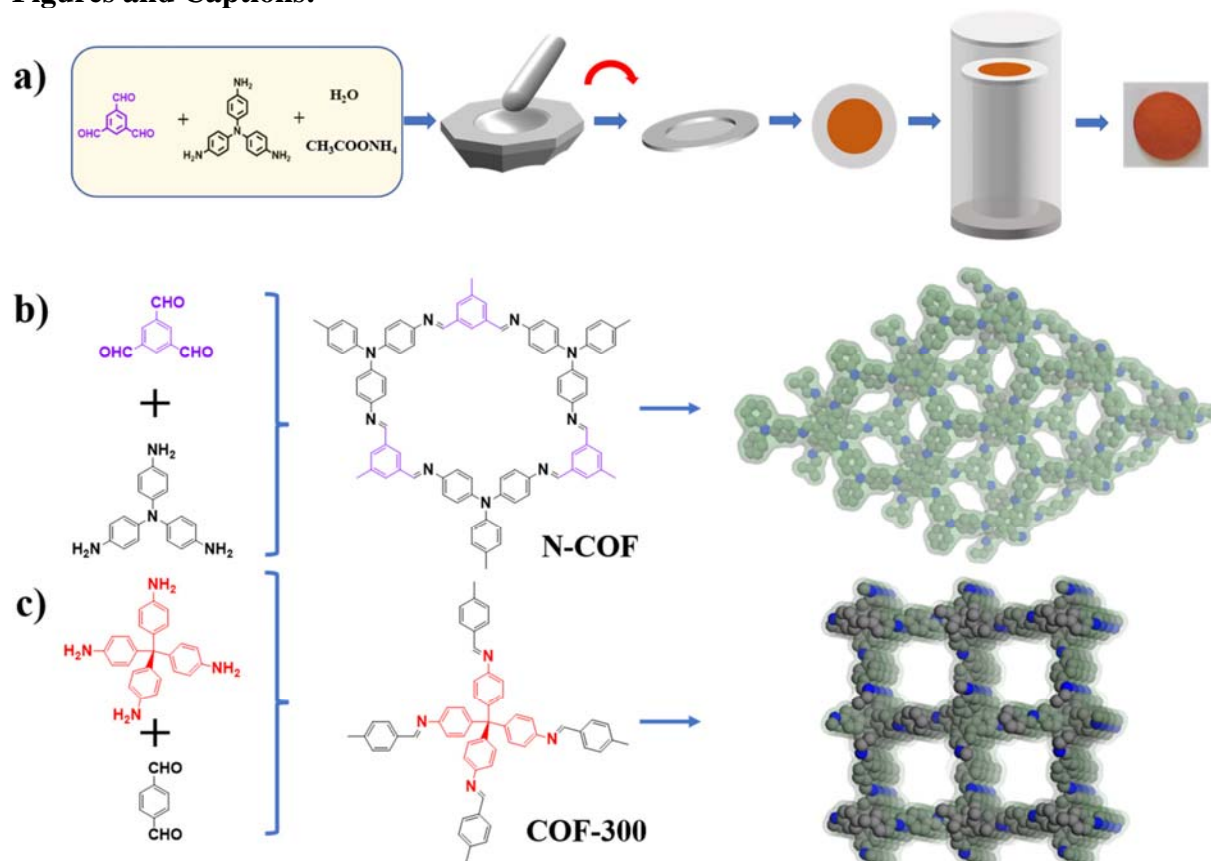
References

- [1] J. Rogelj, M. den Elzen, N. Höhne, T. Fransen, H. Fekete, H. Winkler, R. Schaeffer, F. Sha, K. Riahi, M. Meinshausen, *Nature* **2016**, *534*, 631.
- [2] N. W. Ockwig, T. M. Nenoff, *Chem. Rev.* **2007**, *107*, 4078.
- [3] H. Dou, M. Xu, B. Wang, Z. Zhang, G. Wen, Y. Zheng, D. Luo, L. Zhao, A. Yu, L. Zhang, Z. Jiang, Z. Chen, *Chem. Soc. Rev.* **2021**, *50*, 986.
- [4] Z. Kang, H. Guo, L. Fan, G. Yang, Y. Feng, D. Sun, S. Mintova, *Chem. Soc. Rev.* **2021**, *50*, 1913.
- [5] W. J. Koros, C. Zhang, *Nat. Mater.* **2017**, *16*, 289.
- [6] A. P. Cote, A. I. Benin, N. W. Ockwig, M. O'Keeffe, A. J. Matzger, O. M. Yaghi, *Science* **2005**, *310*, 1166.
- [7] H. M. El-Kaderi, J. R. Hunt, J. L. Mendoza-Cortes, A. P. Cote, R. E. Taylor, M. O'Keeffe, O. M. Yaghi, *Science* **2007**, *316*, 268.
- [8] F. Q. Chen, X. Y. Guan, H. Li, J. H. Ding, L. K. Zhu, B. Tang, V. Valtchev, Y. S. Yan, S. L. Qiu, Q. R. Fang, *Angew. Chem., Int. Ed.* **2021**, *60*, 22230.
- [9] Y. Yusran, H. Li, X. Guan, D. Li, L. Tang, M. Xue, Z. Zhuang, Y. Yan, V. Valtchev, S. Qiu, Q. Fang, *Adv. Mater.* **2020**, *32*, 1907289.

- [10] Q. Fang, Z. Zhuang, S. Gu, R. B. Kaspar, J. Zheng, J. Wang, S. Qiu, Y. Yan, *Nat. Commun.* **2014**, *5*, 4503.
- [11] L. Chen, K. Furukawa, J. Gao, A. Nagai, T. Nakamura, Y. Dong, D. Jiang, *J. Am. Chem. Soc.* **2014**, *136*, 9806.
- [12] H. Li, F. Chen, X. Guan, J. Li, C. Li, B. Tang, V. Valtchev, Y. Yan, S. Qiu, Q. Fang, *J. Am. Chem. Soc.* **2021**, *143*, 2654.
- [13] Z. Wang, S. Zhang, Y. Chen, Z. Zhang, S. Ma, *Chem. Soc. Rev.* **2020**, *49*, 708.
- [14] R. Liu, K. T. Tan, Y. Gong, Y. Chen, Z. Li, S. Xie, T. He, Z. Lu, H. Yang, D. Jiang, *Chem. Soc. Rev.* **2021**, *50*, 120.
- [15] Q. Hao, C. Zhao, B. Sun, C. Lu, J. Liu, M. Liu, L. J. Wan, D. Wang, *J. Am. Chem. Soc.* **2018**, *140*, 12152.
- [16] D. B. Shinde, G. Sheng, X. Li, M. Ostwal, A. H. Emwas, K. W. Huang, Z. Lai, *J. Am. Chem. Soc.* **2018**, *140*, 14342.
- [17] K. Dey, M. Pal, K. C. Rout, H. S. Kunjattu, A. Das, R. Mukherjee, U. K. Kharul, R. Banerjee, *J. Am. Chem. Soc.* **2017**, *139*, 13083.
- [18] P. Wang, Y. Peng, C. Zhu, R. Yao, H. Song, L. Kun, W. Yang, *Angew. Chem., Int. Ed.* **2021**, *60*, 19047.
- [19] N. A. Khan, R. Zhang, H. Wu, J. Shen, J. Yuan, C. Fan, L. Cao, M. A. Olson, Z. Jiang, *J. Am. Chem. Soc.* **2020**, *142*, 13450.
- [20] H. S. Sasmal, S. Bag, B. Chandra, P. Majumder, H. Kuiry, S. Karak, S. Sen Gupta, R. Banerjee, *J. Am. Chem. Soc.* **2021**, *143*, 8426.
- [21] S. Mohata, K. Dey, S. Bhunia, N. Thomas, E. B. Gowd, T. G. Ajithkumar, C. M. Reddy, R. Banerjee, *J. Am. Chem. Soc.* **2022**, *144*, 400.
- [22] A. Kumar Mahato, S. Bag, H. S. Sasmal, K. Dey, I. Giri, M. Linares-Moreau, C. Carbonell, P. Falcaro, E. B. Gowd, R. K. Vijayaraghavan, R. Banerjee, *J. Am. Chem. Soc.* **2021**, *143*, 20916.
- [23] K. Dey, S. Bhunia, H. S. Sasmal, C. M. Reddy, R. Banerjee, *J. Am. Chem. Soc.* **2021**, *143*, 955.
- [24] H. Fan, A. Mundstock, A. Feldhoff, A. Knebel, J. Gu, H. Meng, J. Caro, *J. Am. Chem. Soc.* **2018**, *140*, 10094.
- [25] Y. Ying, S. B. Peh, H. Yang, Z. Yang, D. Zhao, *Adv. Mater.* **2021**, 2104946.
- [26] J. Fu, S. Das, G. Xing, T. Ben, V. Valtchev, S. Qiu, *J. Am. Chem. Soc.* **2016**, *138*, 7673.
- [27] H. Fan, M. Peng, I. Strauss, A. Mundstock, H. Meng, J. Caro, *J. Am. Chem. Soc.* **2020**, *142*, 6872.
- [28] H. Fan, M. Peng, I. Strauss, A. Mundstock, H. Meng, J. Caro, *Nat. Commun.* **2021**, *12*, 38.
- [29] Y. J. Zhao, P. Liu, Y. P. Ying, K. P. Wei, D. Zhao, D. H. Liu, *J. Membr. Sci.* **2021**, *632*, 119326.
- [30] H. Fan, J. Gu, H. Meng, A. Knebel, J. Caro, *Angew. Chem., Int. Ed.* **2018**, *57*, 4083.
- [31] X. Shi, A. Xiao, C. Zhang, Y. Wang, *J. Membr. Sci.* **2019**, *576*, 116.
- [32] Z. Wang, Z. H. Si, D. Cai, G. Z. Li, S. F. Li, P. Y. Qin, *J. Membr. Sci.* **2020**, *615*, 118466.
- [33] J. M. Rotter, S. Weinberger, J. Kampmann, T. Sick, M. Shalom, T. Bein, D. D. Medina, *Chem. Mater.* **2019**, *31*, 10008.
- [34] P. Manchanda, S. Chisca, L. Upadhyaya, V.-E. Musteata, M. Carrington, S. P. Nunes, *J. Mater. Chem. A* **2019**, *7*, 25802.
- [35] H. S. Sasmal, H. B. Aiyappa, S. N. Bhange, S. Karak, A. Halder, S. Kurungot, R. Banerjee, *Angew. Chem., Int. Ed.* **2018**, *57*, 10894.
- [36] J. A. Martin-Illan, J. A. Suarez, J. Gomez-Herrero, P. Ares, D. Gallego-Fuente, Y. Cheng, D. Zhao, D. Maspoch, F. Zamora, *Adv. Sci.* **2022**, 2104643.

- [37] S. Kandambeth, B. P. Biswal, H. D. Chaudhari, K. C. Rout, H. S. Kunjattu, S. Mitra, S. Karak, A. Das, R. Mukherjee, U. K. Kharul, R. Banerjee, *Adv. Mater.* **2017**, *29*, 1603945.
- [38] *Materials Studio ver. 7.0*; Accelrys Inc.: San Diego, CA, **2013**.
- [39] J. Q. Dong, Y. X. Wang, G. L. Liu, Y. D. Cheng, D. Zhao, *Crystengcomm* **2017**, *19*, 4899.
- [40] F. J. Uribe-Romo, J. R. Hunt, H. Furukawa, C. Klock, M. O'Keeffe, O. M. Yaghi, *J. Am. Chem. Soc.* **2009**, *131*, 4570.
- [41] N. Wang, Y. Liu, Z. Qiao, L. Diestel, J. Zhou, A. Huang, J. Caro, *J. Mater. Chem. A* **2015**, *3*, 4722.
- [42] F. Zhang, X. Zou, X. Gao, S. Fan, F. Sun, H. Ren, G. Zhu, *Adv. Funct. Mater.* **2012**, *22*, 3583.
- [43] W. Zheng, J. Hou, C. Liu, P. Liu, L. Li, L. Chen, Z. Tang, *Chem. Asian. J.* **2021**, *16*, 3624.
- [44] L. M. Robeson, *J. Membr. Sci.* **2008**, *320*, 390.
- [45] L. Li, Y. Duan, S. Liao, Q. Ke, Z. Qiao, Y. Wei, *Chem. Eng. J.* **2020**, *386*, 123945.
- [46] J. Fu, T. Ben, *Acta Chimica Sinica* 2020, *78*, 805.
- [47] Y. Ying, M. Tong, S. Ning, S. K. Ravi, S. B. Peh, S. C. Tan, S. J. Pennycook, D. Zhao, *J. Am. Chem. Soc.* 2020, *142*, 4472.

Figures and Captions:



Scheme 1. (a) Schematic representation of the COFM fabrication. (b,c) Structure and composition of N-COF membrane (b) and COF-300 membrane (c).

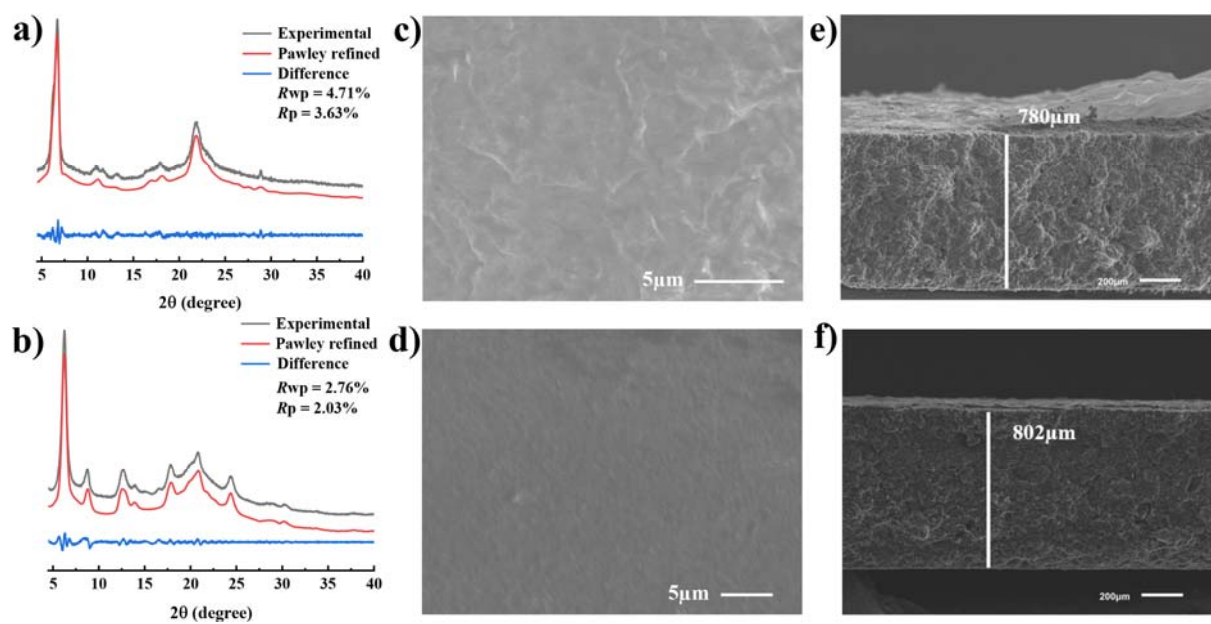


Figure 1. (a,b) PXRD patterns of N-COF membrane (a) and COF-300 membrane (b). (c,d) SEM images showing the surfaces of N-COF membrane (c) and COF-300 membrane (d). (e,f) Cross-section SEM images of N-COF membrane (e) and COF-300 membrane (f).

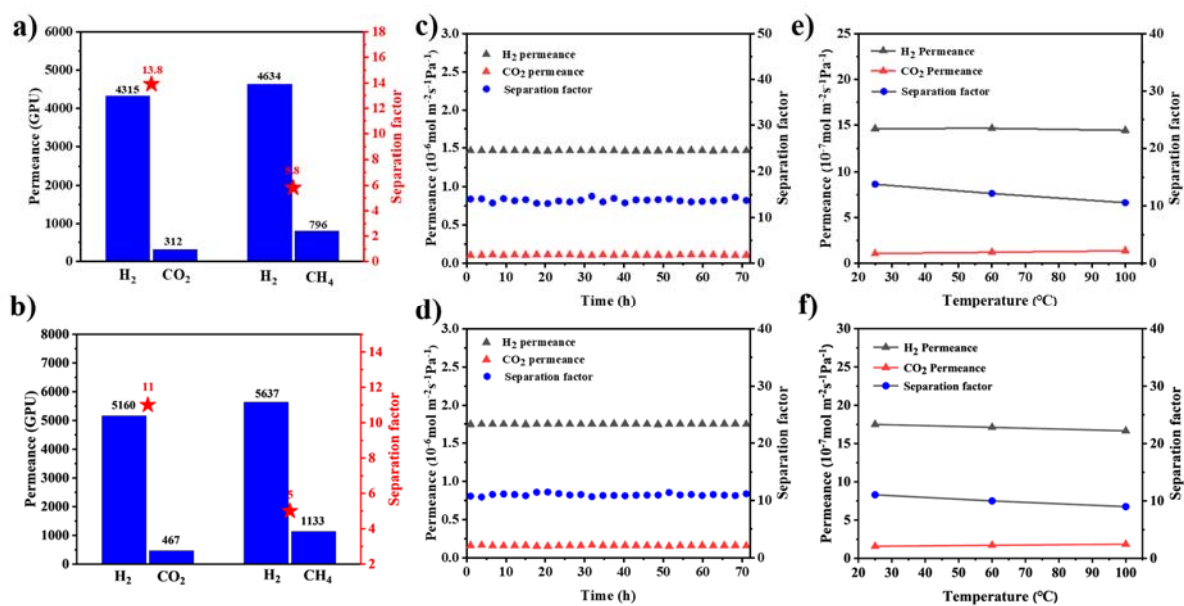


Figure 2. (a,b) Equimolar binary gas mixture separation performance of N-COF membrane (a) and COF-300 membrane (b). (c,d) Long-term test of N-COF membrane (c) and COF-300 membrane (d) for equimolar H₂/CO₂ mixture at normal temperature. (e,f) Selectivity and permeances of N-COF membrane (e) and COF-300 membrane (f) as a function of temperature.

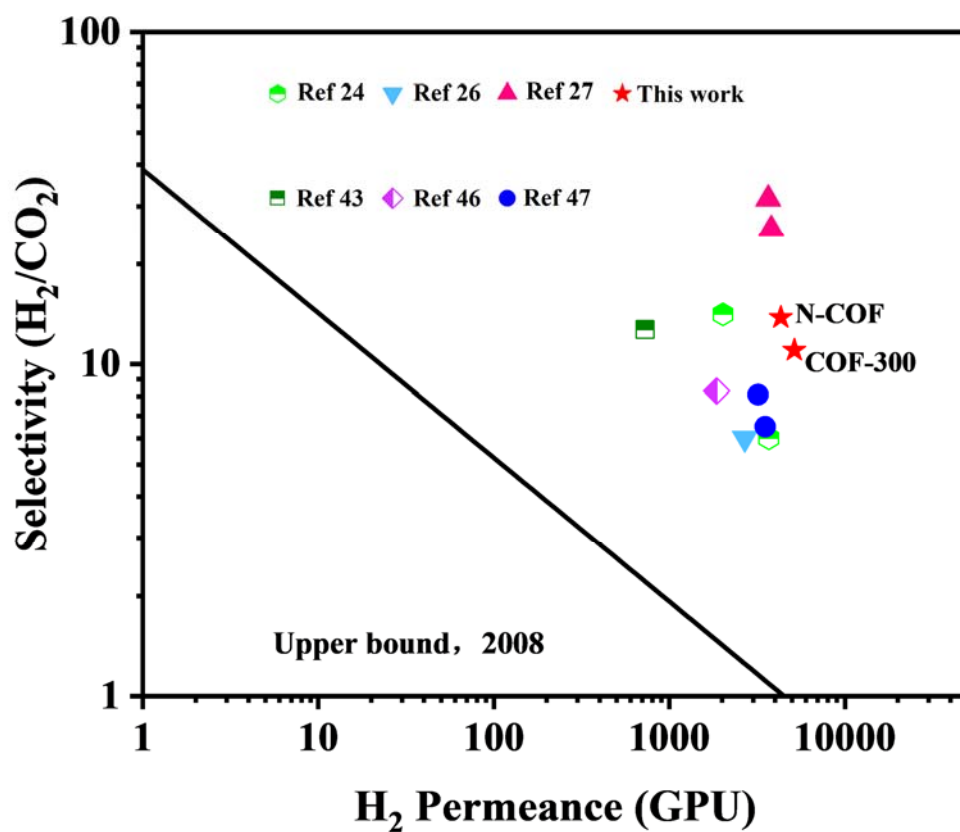


Figure 3. A comparison of H₂/CO₂ selectivity and H₂ permeance for single-phase COFMs reported so far (the details of the H₂/CO₂ separation performance are shown in Table S1).

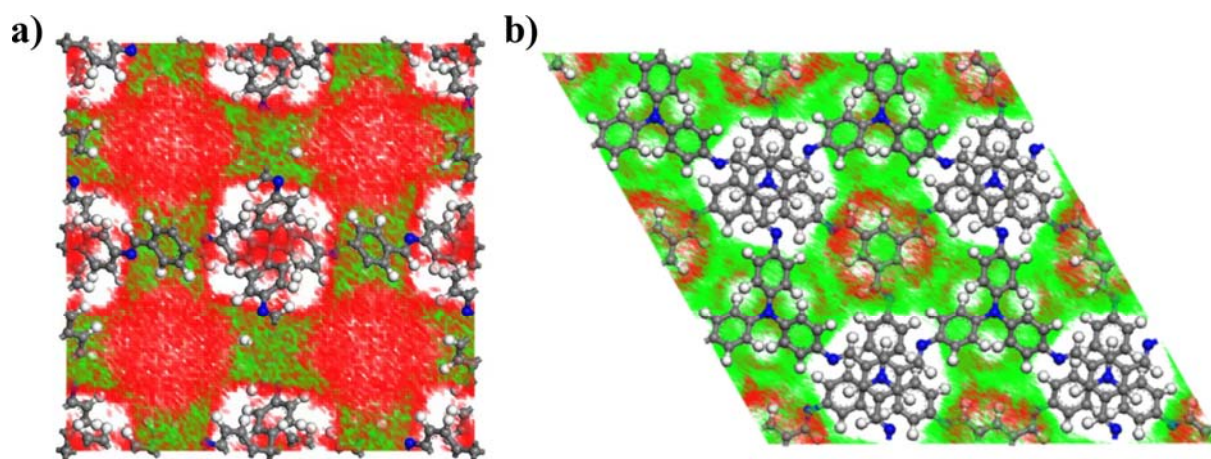


Figure 4. Density distribution contours of H₂ (red) and CO₂ (green) mixture gas in COF-300 membrane (a) and N-COF membrane (b) based on GCMC simulation.

TOC

